REPORT
doi:10.26443/seismica.v4i2.1773

23 April 2025 Marmara Sea (M_w 6.3), Türkiye earthquake: mainshock, aftershock, and ground observations

Deniz Ertuncay * [1], **Pınar Büyükakpınar** [2], **Simone Francesco Fornasari** [3], **Onur Tan** [4]

[1]National Institute of Oceanography and Applied Geophysics - OGS, Trieste, Italy, [2]GFZ Helmholtz Centre for Geosciences, Potsdam, Germany, [3]Department of Mathematics, Informatics, and Geosciences, SeisRaM Working Group, University of Trieste, Trieste, Italy, [4]Department of Geophysical Engineering, University of Istanbul-Cerrahpaşa, Istanbul, Türkiye

Author contributions: *Conceptualization*: Deniz Ertuncay, Pınar Büyükakpınar. *Methodology*: Simone Francesco Fornasari, Onur Tan, Pınar Büyükakpınar. *Software*: Deniz Ertuncay, Simone Francesco Fornasari, Onur Tan, Pınar Büyükakpınar. *Validation*: Deniz Ertuncay, Simone Francesco Fornasari, Onur Tan, Pınar Büyükakpınar. *Formal Analysis*: Deniz Ertuncay, Simone Francesco Fornasari, Pınar Büyükakpınar. *Investigation*: Deniz Ertuncay, Pınar Büyükakpınar. *Resources*: Deniz Ertuncay, Onur Tan, Pınar Büyükakpınar. *Writing - Original draft*: Deniz Ertuncay, Simone Francesco Fornasari, Onur Tan, Pınar Büyükakpınar. *Writing - Review & Editing*: Deniz Ertuncay, Simone Francesco Fornasari, Onur Tan, Pınar Büyükakpınar. *Visualization*: Deniz Ertuncay, Simone Francesco Fornasari, Pınar Büyükakpınar. *Supervision*: Deniz Ertuncay, Pınar Büyükakpınar. *Project administration*: Deniz Ertuncay.

Abstract On 23 April 2025, a M_w 6.3 earthquake struck the Sea of Marmara near the Kumburgaz segment of the North Anatolian Fault (NAF), triggering over 500 aftershocks within 15 days. This study presents a rapid assessment of the event through aftershock relocation using double-difference technique, full moment tensor inversion of the mainshock, and ground motion analysis. The mainshock exhibited a strike-slip mechanism at a depth of 6 km with a significant non-double-couple component (40%). The aftershocks mostly occurred east of the mainshock, primarily within 10 km depth. Shakemaps derived from ground motion recordings highlight peak ground accelerations exceeding 210 cm/s^2 east of the mainshock in western Istanbul and Modified Mercalli Intensities reaching level 6. The ground motion prediction equation developed for the region slightly underestimated the peak ground motions in short-period pseudo-spectral acceleration (PSA) and peak ground acceleration (PGA). Comparison with Turkish seismic design codes revealed that short-period PSA reached code limits in some stations, raising concerns for structural resilience especially in older buildings in those areas.

Özet (Turkish) 23 Nisan 2025 tarihinde, Marmara Denizi'nde Kuzey Anadolu Fayı'nın (KAF) Kumburgaz segmenti yakınlarında M_w 6,3 büyüklüğünde bir deprem meydana geldi ve 15 gün içinde 500'den fazla artçı depreme neden oldu. Bu çalışma, çift fark tekniği (ing. double difference) kullanılarak artçı sarsıntıların yeniden konumlandırılması, moment tensör ters çözümü ve zemin hareketi analizi yoluyla depremin hızlı bir değerlendirmesini sunmaktadır. Ana deprem, 6km derinlikte ve yanal atımlı bir faylanma gösteren bir fay mekanizması çözümüyle meydana gelmiş ve muhtemelen bölgedeki karmaşık faylanma özellikleri nedeniyle kayda değer bir kuvvet çifti olmayan bileşene (ing. non-double-couple) sahip bir yanal atımlı deprem mekanizması sergilemiştir (40%). Artçı depremler genellikle ana depremin doğusunda ve ilk 10 km derinlikte meydana geldi. Zemin hareketi kayıtlarından elde edilen sarsıntı haritaları, İstanbul'un batısında 210 cm/s^2'yi aşan yer ivmelerini ve Mercalli şiddet ölçeğinde 6 seviyesinde değerler gözlendi. Bölge için geliştirilen yer hareketi tahmin denklemi (ing. ground motion prediction equation), kısa periyotlu en büyük spektral ivmelerde (PSA) ve en büyük zemin ivmesi (PGA) için yaptığı tahminlerde gerçekte ölçülen değerlere göre düşük kalmıştır. Türk sismik tasarım kodlarıyla karşılaştırıldığında, bazı istasyonlarda kısa periyotlu PSA'nın kod sınırlarına ulaştığı görülmüş ve bu özellikle o bölgelerde bulunan eski binaların yapısal dayanıklılığı konusunda endişeler uyandırmıştır.

Production Editor:
Kiran Kumar Thingbaijam
Handling Editor:
Tiegan Hobbs
Copy & Layout Editor:
Hannah F. Mark

Signed reviewer(s):
Tiegan Hobbs

Received:
June 4, 2025
Accepted:
October 20, 2025
Published:
November 10, 2025

1 Introduction

The North Anatolian Fault (NAF) is the Eurasian-Anatolian tectonic plate boundary (Şengör et al., 2005). It is a right-lateral strike-slip fault that accommodates the west-to-southwest Anatolian microplate movement at an average rate of approximately 20 mm/yr (Reilinger et al., 2006). It is induced by the northward nudge of the Arabian plate against the Eurasian plate, forcing the Anatolian plate to escape to the west (Reilinger et al., 2006; Ergintav et al., 2023). NAF has experienced numerous large earthquakes ($M > 7$) in the last 100 years (Ambraseys, 2002), including notable events in 1939 (Erzincan, M 7.8) and 1999 (Izmit, M 7.4).

The Marmara Region, located in northwestern Türkiye, is an active tectonic zone where the NAF crosses beneath the Sea of Marmara. The area has witnessed damaging earthquakes in the 20th century, such as the 1912 Mürefte (surface wave magnitude, M_s 7.3; Aksoy et al., 2010) and 1999 (moment magnitude, M_w 7.4) Izmit earthquakes (Figure 1). These earthquakes

*Corresponding author: dertuncay@ogs.it

caused extensive damage and highlighted the seismic hazard of the region (Karasözen et al., 2023; Erdik et al., 2025), especially due to its proximity to the densely populated megacity of Istanbul (Figure 1).

During the 20th century, most of the NAF segments ruptured in major earthquakes, except for the western segments beneath the Sea of Marmara, along the so-called Main Marmara Fault (MMF), located near Istanbul (Le Pichon et al., 2001). The presence of a seismic gap in the MMF, between the rupture zones of 1912 and 1999 in the Sea of Marmara, has long been a topic of debate, as the theory suggests that this unbroken section could produce a major earthquake (M > 7) (Bohnhoff et al., 2013; Ergintav et al., 2014; Öztürk et al., 2025). Recent studies have revealed that parts of this region undergo aseismic creep, rather than sudden rupture, particularly along the Tekirdağ and Central Basins (Bohnhoff et al., 2013). The Marmara Sea has historically experienced many large earthquakes, and the Kumburgaz, Çınarcık, and Princes' Island segments (Figure 1) were expected to rupture due to an overdue seismic gap in the regional seismic cycling (Schmittbuhl et al., 2016).

Relative to other parts of the NAF, the MMF beneath the Sea of Marmara has a more complex structure. It displays many sub-faults (Emre et al., 2018), characterized by multiple subsidiary faults of different orders, ranging from small to large. This raises questions about whether stress is distributed across numerous faults in a wider zone or concentrated along the principal fault zone (Figure 1). The tectonic complexity of the area is added to by the presence of a pull-apart basin, crustal thinning, and locally thick sedimentary deposits up to 7 km in the western Marmara Sea (Yılmaz et al., 2022; Bécel et al., 2009), which may be important controlling factors influencing the potential for large earthquakes in the region.

The Sea of Marmara had not witnessed a major earthquake (M>7) or greater during the instrumental period, but it produced moderate earthquakes. The M_w 5.8 Silivri earthquake that occurred in September 2019, only a few kilometers from the Kumburgaz Basin (Karabulut et al., 2021) and had a complex source mechanism (Şahin et al., 2022; Turhan et al., 2023). Karabulut et al. (2021) demonstrated that the 2019 thrust fault mechanism of the earthquake, the spatial and temporal distribution of its aftershocks, and the accompanying stress changes could plausibly have increased the overall stress along the Marmara Fault segment. Aftershocks primarily propagated southeast, where the largest slip was also observed, near the MMF. Using a finite-fault model derived from strong-motion data, Karabulut et al. (2021) calculated Coulomb stress changes and found that the Silivri earthquake increased stress, particularly in the southeastern portion of the rupture zone, at depths of 7–10 km. This area lies along the MMF, in the transition between the Central and Kumburgaz Basins.

Istanbul is one of the most populous cities in the world, with a high seismic hazard and risk due to the NAF's capability of producing large-magnitude earthquakes (Şengör et al., 2005). A supposed seismic gap located in the south of Istanbul, in the Marmara Sea, makes Istanbul one of the most studied cities in terms of hazard (Atakan et al., 2002; Akinci et al., 2017; Infantino et al., 2020) and risk (Pyper Griffiths et al., 2007; Yakut et al., 2012; Stupazzini et al., 2021). The current seismic design code of Türkiye estimates its design limits using prescribed short, medium, and long spectral periods that are assessed via empirical ground motions prediction equations (Akkar et al., 2018). Hence, estimating ground motion parameters and spectral amplitudes plays a significant role in understanding the performance of the current design code, as well as in estimating damage states for structures built according to design criteria for regular (residential and commertial) and strategic buildings (schools, governmental buildings etc.) which use 10% and 2% probability of exceedance in 50 years to determine the amplitudes of the design code, respectively.

Peak ground motions also carry important information regarding the earthquake physics, as the directivity effect carries large amplitudes with long periods towards the propagation direction (Somerville et al., 1997), and permanent ground deformation (fling step effect) may produce large seismic loads, especially to tall structures (Kenawy and Pitarka, 2025). Local site effects may also amplify the ground motions (Klin et al., 2021), which may amplify the destructive effects of earthquakes (Özel et al., 2002). Thus, estimating ground motion variations in a seismic event is crucial for assessing earthquake physics, shallow soil effects, and damage distribution.

On 23 April 2025 at 09:49:16 (UTC), a M_w 6.3 earthquake struck the Sea of Marmara. Here we assess the mainshock and aftershocks, relocate over 550 aftershocks within the first 15 days, and investigate the full moment tensor of the main shock. Furthermore, we create shakemaps to find the spatial distribution of ground motions, plot ground motion parameters compared with a regional attenuation model, and compare the spectral response at near-epicentral stations with several Turkish seismic design codes. Finally, we discuss the seismic significance of this earthquake relative to the Marmara Sea and emphasise key questions raised by this event.

2 Data

For the relocation analysis, a seismic catalog, which contains 562 aftershocks between 23 April and 9 May 2025, is obtained from the Disaster and Emergency Management Authority (1973) event catalog database. For the full moment tensor (MT) inversion of the mainshock, open access seismic data from nine different regional networks (see the Data and code availability), with station distances ranging between 250 and 900 km, were inverted after a visual quality check using the Pyrocko/Snuffler (Heimann et al., 2017) software. Waveforms with large time gaps, clipping, or excessive noise were excluded from the analysis. In total, 20 three-component stations were selected for MT inversion, and the waveforms were rotated into the radial (R), transverse (T), and vertical (Z) components. The CRUST2.0

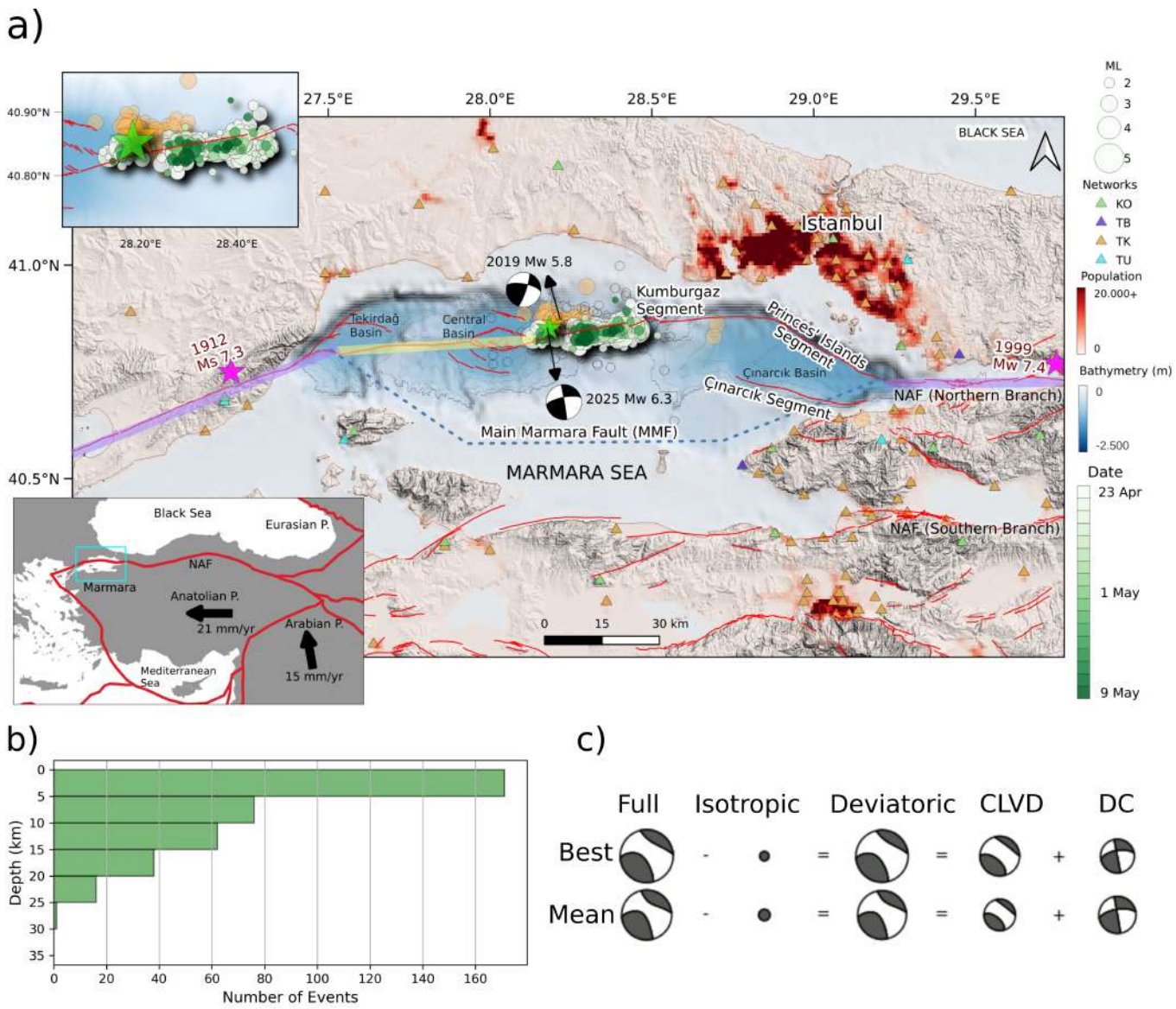

Figure 1 **a)** Map of the Marmara region and the features in the Marmara Sea. The figure displays the 23 April 2025 M_w 6.3 earthquake source mechanism and its aftershock distribution (green dots, aftershocks relocated in this study). The green star shows the centroid location of the mainshock. The triangles indicate the stations used in this study. The red lines show the active fault lines in the region (Emre et al., 2018), including the Kumburgaz, Çınarcık, and Princes' Islands segments (labelled). The seismic activity is plotted for the comparison of the two seismic sequences. Black circles indicate outliers according to our relocation criteria (see Section 3.1). The orange star shows the centroid location of the 26 September 2019, M_w 5.8 earthquake (Karabulut et al., 2021) and its aftershocks, which are shown by orange circles. The bottom-left inset shows the regional tectonic setting, including plate boundaries and relative plate motions (Reilinger et al., 2006). The top-left inset shows a zoom-in of the aftershock distributions for both sequences. The ruptured segments and the locations of the 1912 and 1999 earthquakes are given in magenta. The yellow highlighted area shows the segment of transition and the creeping (aseismic part) by Becker et al. (2023). **b)** Depth distribution of the aftershocks in histograms. **c)** The decomposition of full Moment Tensor inversion for the best and mean solutions for the 2025 mainshock. The symbol size indicates the relative strength of the components.

velocity model (Bassin et al., 2000) was used for these inversions.

The seismic data for the ground motion analysis is obtained from the national networks of Disaster and Emergency Management Authority (1973, 1990); Kandilli Observatory And Earthquake Research Institute, Boğaziçi University (1971); TÜBITAK Marmara Research Center (2016). In total, data from 262 stations with epicentral distances (R_{epi}) between 25 - 220 km are used in which 224 have good data quality. Many broadband stations suffered from saturation effects and are excluded from further processing. In total, 22 broadband and 202 strong motion recordings were identified for the ground motion assessment.

3 Methods

3.1 Earthquake Relocation

The events are analyzed using the hypoDD double-difference (DD) inversion algorithm (Waldhauser and Ellsworth, 2000) following similar steps, such as event selection, phase weighting, and uncertainty determination, presented by Tan et al. (2023) and Tan (2024) and using the 1D velocity model developed by Karabulut et al. (2011). The algorithm assumes that the hypocentral separation between two neighboring events is smaller than the station distances. Therefore, the ray paths are similar, and the travel time difference between two events observed at a common station can be attributed to the spatial offset between the events (Got et al., 1994; Waldhauser and Ellsworth, 2000). The ten nearest neighboring events within a 5 km radius, considering the aftershock distribution, are selected to construct event-pair chains for a robust DD inversion. The minimum 8 P/S phase arrival time observations are used to generate event pairs. According to these criteria, about 545 events are selected for the DD inversion and about 400 events are relocated.

3.2 Moment Tensor Inversion

We performed full MT inversion based on a Bayesian bootstrap probabilistic joint inversion method using the Grond software (Heimann et al., 2018; Büyükakpınar et al., 2022; Metz et al., 2023; Jamalreyhani et al., 2023). This method provides the uncertainties for the model parameters of the resulting MT inversion. The source model parameterization consists of the location, depth, and time of the point-like earthquake origin (centroid), the six independent components of the moment tensor, and a source duration. The MT was calculated via waveform inversion in the time domain using three-component data (R, T, and Z) in the frequency band of 0.02–0.05 Hz to invert the surface waves, with the frequency band chosen based on the event magnitude and station distance, as further details can be found in Kühn et al. (2020). Synthetic seismograms were taken from pre-calculated Green's functions (Heimann et al., 2019). We applied 50,000 iterations for a robust inversion based on convergence tests. The inversion provides the best and mean solutions, as well as uncertainties in the source parameters.

3.3 Ground Motion Parameters and Intensity Distribution

To estimate the ground motions, instrument response removal, detrending, Hann window tapering with a 5% taper ratio, and filtering with 4th-order Butterworth bandpass filtering between 0.01 - 50 Hz have been applied to each trace. Ground-shaking maps and the corresponding macroseismic intensity (in terms of Modified Mercalli Intensity, MMI) distribution were generated using ShakeMap (version 4; Wald and Worden, 2016; Worden et al., 2018). Inputs are the peak ground motion parameters: peak ground acceleration (PGA) and peak pseudo-spectral acceleration (under the assumption of single degree of freedom system with 5% damping ratio, PSA), at 0.3s and 1.0s, recorded at 224 seismic stations. For each station, the maximum of the horizontal component is used as input. The ground motion prediction equation (GMPE) by Kale et al. (2015) and the ground motion to intensity conversion equation (GMICE) by Worden et al. (2012) were selected in ShakeMap's configuration to inform the ground motion interpolation. Spatial correlation between ground-motion pseudo-spectral accelerations at different periods was incorporated through the equation (42) by Loth and Baker (2013, 2020). Site effects were accounted for using a Vs_{30} proxy, based on the map developed by Okay and Özacar (2024), unless the site characteristics were determined by Disaster and Emergency Management Authority (1973). The interpolations have been performed under the point-source approximation, considering the hypocentre obtained with the earthquake relocation. The choice has been made considering the distance of the seismic source from the coast, the relatively high density of stations in the area, and the limited effect that the use of an extended source would have with respect to the associated uncertainty.

4 Results

The aftershocks are concentrated east of the epicentre of the mainshock, within the Kumburgaz Basin (Figure 1), at shallow depths, mainly in the top 10 km, with horizontal and vertical uncertainties of ±1.5 km and ±4.4 km, respectively. This eastern clustering resembles the 2019 event, which also showed a similar pattern (Figure 1a top left inset). Karabulut et al. (2021) reported a rupture asymmetry in 2019, with enhanced slip and seismicity to the east. The 2025 aftershocks similarly align with this eastern edge, where stress had previously accumulated, suggesting a comparable concentration mechanism.

The mainshock had a M_w of 6.3 ± 0.2 and was located at 40.86°N, 28.18°E with a 2.5 km epicentral uncertainty. The mean full moment tensor solution indicates a strike-slip mechanism with strike1 = 260°, dip1 = 65°, rake1 = 180°, and strike2 = 350°, dip2 = 90°, rake2 = 25°, with a centroid depth of 6.0 km ± 0.8 km. Non-double couple components are found as isotropic 5% ± 8 and compensated linear vector dipole (CLVD) 40% ± 20. Our results are in good agreement with fault parameters reported by other agencies (e.g., GCMT, USGS, GFZ). Reported focal depths range between 4 km (IPGP, IPGP Data Center, 2024) and 13 km (KOERI, Kandilli Observatory And Earthquake Research Institute, Boğaziçi University, 1971). Significant non-double-couple (non-DC) components have been reported as well, such as USGS 43% (U.S. Geological Survey, Earthquake Hazards Program, 2017), and GCMT 33% (Dziewonski et al., 1981; Ekström et al., 2012). Uncertainties in source parameters e.g., magnitude, depth, and moment tensor components, are systematically reported in our study, providing a more robust interpretation of the source characteristics. An interactive online report showing the results of MT inversion (e.g., uncertainties, waveform fits) is provided in the Data Availability section.

The interpolated ground shaking maps, based on recorded ground motion parameters, are presented in Figure 2 in terms of PGA, PSA at 0.3s and 1.0s, and estimated macroseismic intensity (expressed as MMI). The highest ground motion values on land are observed along the northern coastline near the epicentre and in the area west of Istanbul, in agreement with maximum station recordings. The elevated values recorded at the stations in these areas can be justified by either the closer proximity to the epicentre or the effect of site amplification, as suggested by low Vs_{30} values at stations TK-3415, TK-3416, and TK-3428 (Figure 2h and Figure S1). The instrumental macroseismic intensity exceeds level 6 along the coast and decays gradually with increasing distance from the epicentre. These intensities are not obtained as direct observations of the effects of the earthquake but rather by converting recorded ground motion parameters, and as such, they are expressed as a continuous scale. Given the offshore location of the event and the dense station coverage, the use of a point-source approximation is considered appropriate for this analysis.

Along with the spatial distribution of the ground shaking, the performance of the GMPE model developed for the region by Kale et al. (2015) is also evaluated, which provides essential information regarding the attenuation trends in the area. Kale et al. (2015)'s model slightly underestimated the PGA and PSA 0.3s (Figure 2), whereas in PSA 1.0s the predictions of the model overestimates the observations. Residuals of the GMPE model can be seen in Supplementary Material (Figure S2).

We carry out a further analysis on the spectral acceleration data to understand the performance of current and previous Turkish design codes. Following the 1939 Erzincan earthquake (M_w 7.9) in Türkiye, the first earthquake design principles were introduced at the national level, along with the country's earthquake hazard maps. The first modern design code was introduced in 1975, then it was updated in 1997, 2007, and 2018 (Akkar et al., 2018; Büyüksaraç et al., 2022). We selected stations of TK-3415, TK-3929, TK-3431, and TK-5906 to compare the design codes as they are either the stations closest to the epicentre and/or those that recorded the largest PGA (Figure 2). For the analysed signals and locations, the design codes have spectral amplitudes between 0.75g and 1.2g, depending on the design code, in the intermediate frequencies. As shown in Figure 3, observed spectral amplitudes are lower than the design codes, except for the very low-frequency content of TK-3431, which exceeds the 1997 design code.

5 Discussion

The centroid of the 23 April 2025, Marmara Sea earthquake (M_w 6.3) is on the western edge of the Kumburgaz Basin, south of the epicenter of the 2019 M_w 5.8 earthquake. The earthquake ruptured the Kumburgaz Basin and occurred along the NAF with a strike-slip mechanism at a depth of 6 km, exhibiting a significant CLVD component. This location was anticipated due to stress transfer southward toward the Kumburgaz Basin and closer to the NAF caused by the previous earthquake (Karabulut et al., 2021). The previous event was characterized by a complex source mechanism with high non-DC components (Turhan et al., 2023) as in the case of the 2025 M_w 6.3 event.

The observed CLVD component in the 2025 earthquake could be due to the various factors related to the source process, crustal structure, inversion artifacts, or the data quality. From a source perspective, geometric fault complexities—such as fault steps, bends, or branches—as well as stress heterogeneity and rupture segmentation can generate non-DC radiation (Frohlich et al., 1989; Kuge and Lay, 1994). In terms of structural effects, lateral variations in sediment thickness and crustal anisotropy may distort waveform propagation and contribute to the apparent non-DC component. Seismic anisotropy, in particular, has been documented in the Marmara region (Eken et al., 2013) and should be considered when interpreting moment tensor solutions. From the inversion, complex source-time functions that are not sufficiently represented in the assumed source models can lead to fake CLVD signatures. Inversion artifacts may also result from network geometry, velocity model inaccuracies, or methodological limitations (Rösler et al., 2023, 2024; Büyükakpınar et al., 2025). Lastly, misoriented horizontal components can also produce misleading CLVD features in the MT inversion (Büyükakpınar et al., 2021). The estimation and interpretation of CLVD is delicate and should therefore be approached with caution (Büyükakpınar et al., 2025). While a detailed discrimination of these contributing factors is beyond the scope of this rapid report, further research is warranted.

The aftershocks of the 23 April earthquake were distributed over 40 km along the Kumburgaz Basin. The hypocentral depth ranges from 0 to 20 km mainly in the first 10 km, aligning with the depth of the centroid of the mainshock. Similar to the 2019 Silivri and 1999 Izmit earthquakes, the April 2025 earthquake also exhibited an eastward pattern of aftershocks, consistent with the regional tectonics and right-lateral strike-slip mechanism of the NAF (Karabulut et al., 2021; Becker et al., 2023).

The Marmara Sea has historically experienced many large earthquakes, and the Kumburgaz, Çınarcık, and Princes' Islands were expected to rupture due to an overdue seismic gap in seismic cycling (Schmittbuhl et al., 2016). Interestingly, the Çınarcık Basin has not ruptured, despite several studies speculating that it could produce an M>7 earthquake (Parsons et al., 2000; Erdik et al., 2004). This raises the important question of whether stress barriers and/or another creeping segment may exist in the west. Similar complexities have been observed in the Tekirdağ Basin region to the west, where evidence suggests variable coupling along the fault (Becker et al., 2023). Further studies are needed to better constrain the slip behavior of individual segments along the MMF in light of recent seismic activity.

The large PGA recorded in Silivri district (TK-3429 station, PGA: 106 cm/s^2) can be linked to the epicentre's proximity. On the other hand, large PGA values are observed in stations located on the western part of the city. Districts such as Avcılar (Station TK-3428, PGA: 94

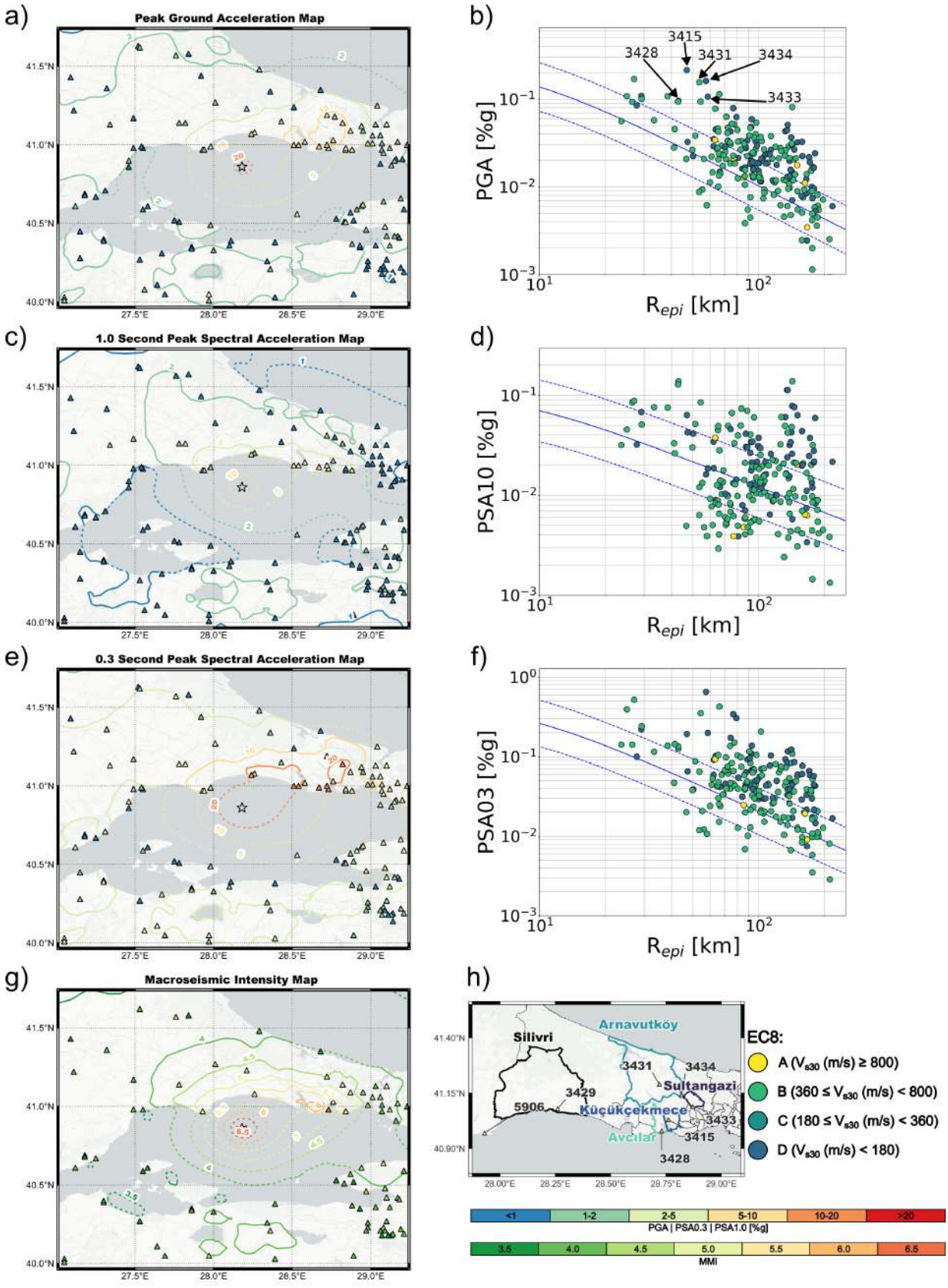

Figure 2 Ground shaking maps for different ground motion parameters and corresponding values at the stations are shown in panels **a)**, **c)**, **e)**, and **g)**. The star represents the epicentre of the point source used during the interpolation. PGA, PSA and MMI are colored according to colorbars shown at the bottom right. Panels **b)**, **d)**, and **f)** show the corresponding observed ground motions at each station compared with the GMPE by Kale et al. (2015), whose median is drawn as a solid blue line and the $\pm$ one standard deviation (σ) as a dashed blue line. Points are colored based on the EC8 site condition category shown in panel h). Station labels in panel b) are shown in map **h)**.

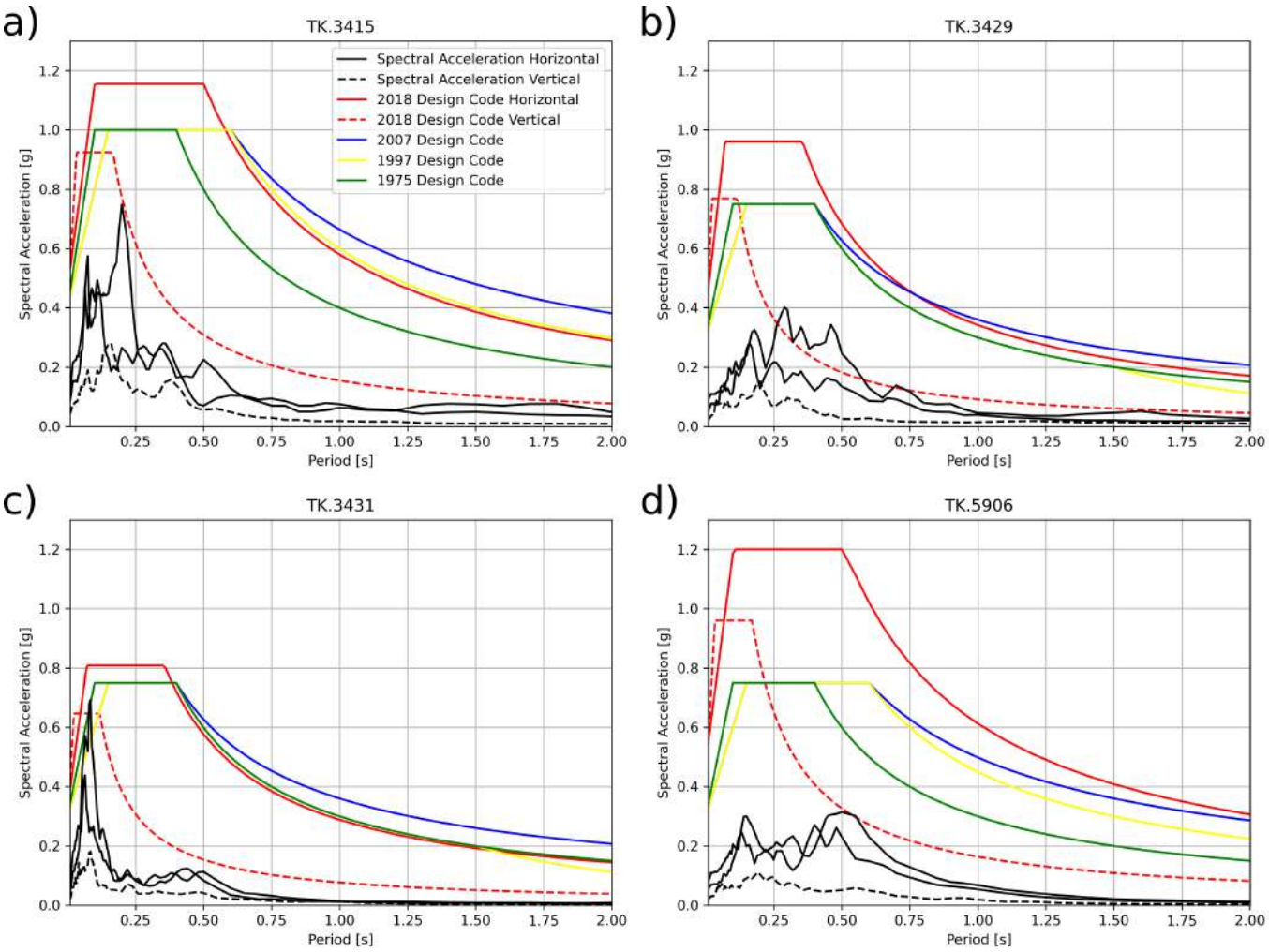

Figure 3 Observed horizontal (solid black line) and vertical (dashed black line) spectral acceleration responses (5% damping) of **a)** TK-3415, **b)** TK-3429, **c)** TK-3431, and **d)** TK-5906. Solid and dashed red lines represent the 2018 Turkish design code's horizontal and vertical design codes, respectively. Blue, yellow, and green lines represent 2007, 1997, and 1975 design codes, respectively.

cm/s^2) and and Küçükçekmece (Station TK-3415, PGA: 210 cm/s^2) are located on an alluvial soil and soil amplification is a well known fact for those areas which also suffered major destruction during August 1999 Izmit earthquake (M_w = 7.4) even though the R_{epi} was around 100km (Ergin et al., 2004; Tezcan et al., 2002; Özel et al., 2002; Kilic et al., 2005; Picozzi et al., 2009; Karabulut and Özel, 2018). Findings of Picozzi et al. (2009) indicate significant site amplification between 0.2 and 10 Hz in the vicinity of TK-3428 and TK-3415, potentially resulting in higher PGAs. Moreover, stations located on the districts north of Avcılar and Küçükçekmece, namely Sultangazi (Station TK-3433, PGA: 105 cm/s^2) and Arnavutköy (Station TK-3431, PGA: 153 cm/s^2, Station TK-3434, PGA: 159 cm/s^2) also recorded large ground motions. These districts experienced rapid urbanisation in the last decade, and soil amplification may play a significant role in the case of a large earthquake; hence, more detailed studies on those parts of the city are essential to understand soil characteristics.

Peak ground motions tend to have larger values along the eastern part of the epicentre, towards Istanbul, with respect to its western part. Apart from the soil amplification, the directivity effect may play a role in the larger amplitudes. Türker et al. (2024) showed a strong directivity effect in 2023 Gölyaka-Düzce Earthquake (M_w = 6.1). Analysing the rupture dynamics can be a good topic for the event to link the large peak ground motions in Istanbul. Large amplitudes in the direction of Istanbul may occur not only due to soil amplification or the directivity effect, but also due to a combination of these two factors.

TK-3429 and TK-5906 stations are some of the closest stations to the epicentre, which is located northeast and northwest of the epicentre. Yet, their spectral acceleration amplitudes are low with respect to the design limits. The energy is concentrated between 0.1s and 0.6s, which is also the case for TK-3415, but in short periods, TK-3415 spectral amplitudes reach almost 0.8g, although the station is far away from the epicentre. In TK-3431, there are large spectral amplitudes in short periods (<0.1s), which is similar to the TK-3415. Large spectral amplitudes at the TK-3431 station approach the design values for all codes within very short periods. The calculated spectral accelerations fall within the capacity range addressed by the current and old seismic design

codes, demonstrating that these codes are sufficiently robust to account for such ground motions.

A major issue with previous design codes was that it used a coarse zonation map to assign amplification factors (Gunes, 2015), which set the design level thresholds at relatively low amplitudes for most of the western side of Istanbul (Akkar et al., 2018). The latest design code incorporates site-specific coefficients to estimate the design code, which are modified from the 2020 European Seismic Hazard Model (Danciu et al., 2021). The combination of low construction quality in old buildings (Cogurcu, 2015), lack of building inspections (Morales-Beltran, 2025), and the ageing effect (Bertolini et al., 2013) results in more than 350 buildings getting structural damage and one building collapsed (Güzel and Fraser, 2025). For an expected large magnitude Marmara earthquake in NAF with a magnitude around 7, old structures will likely suffer significant damage due to the weaknesses mentioned above. It will also be likely to observe underestimated design amplitudes, as observed in the 2023 Kahramanmaraş earthquake doublets (Akinci et al., 2025). If construction standards are not followed, it is possible to expect damage in new buildings as well.

Based on our analysis, we believe some outstanding scientific questions are raised that are given below:

1. To what depth did the rupture associated with the 2025 earthquake and what is the estimated depth extent of fault slip?
2. What are the underlying causes of the source complexity observed in the 2025 earthquake, also observed with the 2019 event, and how is source complexity reflected in the spatial distribution of the aftershocks?
3. How much static stress was transferred to the adjacent fault segments in the Marmara Sea along the NAF following the 2025 rupture, and what is the potential maximum magnitude for the remaining unruptured segments?
4. Can larger amplitudes recorded around Avcılar and western Istanbul be linked to a directivity effect?
5. What is the contribution of the local site amplification on the large ground motions in western Istanbul and are those local site effects not only limited to the Avcılar and its neighbors close to the Marmara Sea, or the same trend can be followed rather north, in Arnavutköy?

6 Conclusions

On 23 April 2025, a M_w 6.3 earthquake occurred on the North Anatolian Fault, underneath the Sea of Marmara, which is capable of creating $M > 7$ earthquakes with an epicentre close to the city of Istanbul on the MMF segment, which is considered to be a seismic gap. The earthquake occurred south of the 2019 M_w 5.8 event with a strike-slip mechanism and more than 500 aftershocks, most of which are positioned on the east side of the epicentre, towards Istanbul. The MT analysis of the main shock shows a considerable CLVD component, which may reflect source and/or structural complexity or heterogeneities within the rupture zone. The earthquake signals are recorded by more than 200 seismic stations (R_{epi} <220km). Ground motion signals have up to 0.2g of PGA and 0.64g in PSA 0.3s. Peak ground motions have larger amplitudes in the northeast of the epicentre (i.e., towards Istanbul) with respect to the northwest direction, which can be due to various factors such as directivity and soil amplification. Although the observed ground motions were close to building code design values at one station, more work is needed to understand patterns of amplification in the west of Istanbul.

Acknowledgements

We would like to thank all seismic data providers to make their data publicly available. We sincerely appreciate all valuable comments and suggestions from the reviewers, which helped us to improve the quality of the manuscript. We also want to thank Fatih Turhan and Ali Özgün Konca from Kandilli Observatory and Regional Tsunami Monitoring Centre of Bogazici University in Türkiye for their help regarding the seismic data. Deniz Ertuncay is funded by the RETURN Extended Partnership and received funding from the European Union Next-GenerationEU (National Recovery and Resilience Plan–NRRP, Mission 4, Component 2, Investment 1.3–D.D. 1243 2/8/2022, PE0000005, CUP F83C22001660002). Pınar Büyükakpınar was funded by the DFG project BU4346/1-1 (project number 517982028).

Data and code availability

Seismic data used in this study are downloaded from the following sources: Disaster and Emergency Management Authority (1973, 1990); Kandilli Observatory And Earthquake Research Institute, Boğaziçi University (1971); TÜBITAK Marmara Research Center (2016); National Institute of Geophysics, Geodesy and Geography - BAS (1980); GEOFON Data Centre (1993); National Observatory of Athens, Institute of Geodynamics, Athens (1975); Aristotle University of Thessaloniki (1981); Geological and Seismological Institute of Moldova (2007); Institutions (1990); National Institute for Earth Physics (NIEP Romania) (1994). Seismic data processing is done with Python packages of ObsPy (Beyreuther et al., 2010), and Pyrocko (Heimann et al., 2017). Ground shaking maps are computed using ShakeMap (Worden et al., 2018). The online interactive report for the moment tensor inversion result of the M_w 6.3 mainshock can be found at https://23april2025marmara-mt.netlify.app/#/. The seismicity movie can be viewed via the following link https://nextcloud.gfz.de/s/SgE26FaZdwzTbxm. Data used in this study are available from Ertuncay et al. (2025), including waveforms and ground motion parameters along with the shakemap outputs. Topography and bathymetry information is obtained from the link https://www.gebco.net/data-products/gridded-bathymetry-data. The plate boundaries are taken from

Hasterok et al. (2022) and population density information is taken from (WorldPop and Bondarenko, 2020) in Figure 1.

Competing interests

The authors declare no competing interests.

References

Akinci, A., Aochi, H., Herrero, A., Pischiutta, M., and Karanikas, D. Physics-based broadband ground-motion simulations for probable Mw≥ 7.0 earthquakes in the Marmara Sea region (Turkey). *Bulletin of the Seismological Society of America*, 107 (3):1307–1323, 2017. doi: 10.1785/0120160096.

Akinci, A., Dindar, A. A., Bal, I. E., Ertuncay, D., Smyrou, E., and Cheloni, D. Characteristics of strong ground motions and structural damage patterns from the February 6th, 2023 Kahramanmaraş earthquakes, Türkiye. *Natural Hazards*, 121(2):1209–1239, 2025. doi: 10.1007/s11069-024-06856-y.

Akkar, S., Azak, T., Can, T., Çeken, U., Demircioğlu Tümsa, M., Duman, T., Erdik, M., Ergintav, S., Kadirioğlu, F., Kalafat, D., et al. Evolution of seismic hazard maps in Turkey. *Bulletin of Earthquake Engineering*, 16:3197–3228, 2018. doi: 10.1007/s10518-018-0349-1.

Aksoy, M., Vallée, M., and Çakir, Z. Rupture characteristics of the AD 1912 Murefte (Ganos) earthquake segment of the North Anatolian Fault (western Turkey). *Geology*, 38:991–994, 11 2010. doi: 10.1130/G31447.1.

Ambraseys, N. The seismic activity of the Marmara Sea region over the last 2000 years. *Bulletin of the Seismological Society of America*, 92(1):1–18, 2002. doi: 10.1785/0120000843.

Aristotle University of Thessaloniki. Aristotle University of Thessaloniki Seismological Network, 1981. doi: 10.7914/SN/HT.

Atakan, K., Ojeda, A., Meghraoui, M., Barka, A. A., Erdik, M., and Bodare, A. Seismic hazard in Istanbul following the 17 August 1999 Izmit and 12 November 1999 Duzce earthquakes. *Bulletin of the Seismological Society of America*, 92(1):466–482, 2002. doi: 10.1785/0120000828.

Bassin, C., Laske, G., and Masters, G. The Current Limits of Resolution for Surface Wave Tomography in North America. *EOS Trans AGU*, 81:F897, 2000.

Becker, D., Martínez-Garzón, P., Wollin, C., Kılıç, T., and Bohnhoff, M. Variation of fault creep along the overdue Istanbul-Marmara seismic gap in NW Türkiye. *Geophysical Research Letters*, 50(6): e2022GL101471, 2023. doi: 10.1029/2022GL101471.

Bertolini, L., Elsener, B., Pedeferri, P., Redaelli, E., and Polder, R. B. *Corrosion of steel in concrete: prevention, diagnosis, repair*. John Wiley & Sons, 2013.

Beyreuther, M., Barsch, R., Krischer, L., Megies, T., Behr, Y., and Wassermann, J. ObsPy: A Python toolbox for seismology. *Seismological Research Letters*, 81(3):530–533, 2010. doi: 10.1785/gssrl.81.3.530.

Bohnhoff, M., Bulut, F., Dresen, G., Malin, P. E., Eken, T., and Aktar, M. An earthquake gap south of Istanbul. *Nature communications*, 4(1):1999, 2013. doi: 10.1038/ncomms2999.

Büyüksaraç, A., Işık, E., and Bektaş, Ö. A comparative evaluation of earthquake code change on seismic parameter and structural analysis; a case of Turkey. *Arabian Journal for Science and Engineering*, 47(10):12301–12321, 2022. doi: 10.1007/s13369-022-07099-4.

Bécel, A., Laigle, M., de Voogd, B., Hirn, A., Taymaz, T., Galvé, A., Shimamura, H., Murai, Y., Lépine, J.-C., Sapin, M., and Özalaybey, S. Moho, crustal architecture and deep deformation under the North Marmara Trough, from the SEISMARMARA Leg 1 offshore–onshore reflection–refraction survey. *Tectonophysics*, 467(1):1–21, 2009. doi: 10.1016/j.tecto.2008.10.022.

Büyükakpınar, P., Aktar, M., Petersen, G., and Köseoğlu, A. Orientations of Broadband Stations of the KOERI Seismic Network (Turkey) from Two Independent Methods: P- and Rayleigh-Wave Polarization. *Seismological Research Letters*, 92(3):1512–1521, 2021. doi: 10.1785/0220200362.

Büyükakpınar, P., Cannata, A., Cannavò, F., Carbone, D., De Plaen, R. S. M., Di Grazia, G., King, T., Lecocq, T., Liuzzo, M., and Salerno, G. Chronicle of Processes Leading to the 2018 Eruption at Mt. Etna As Inferred by Seismic Ambient Noise Along With Geophysical and Geochemical Observables. *Journal of Geophysical Research: Solid Earth*, 127(10):e2022JB025024, 2022. doi: 10.1029/2022JB025024.

Büyükakpınar, P., Isken, M. P., Heimann, S., Dahm, T., Kühn, D., Starke, J., López Comino, J. Á., Cesca, S., Doubravová, J., Gudnason, E. Á., and Ágústsdóttir, T. Understanding the seismic signature of transtensional opening in the Reykjanes Peninsula rift zone, SW Iceland. *J. Geophys. Res.*, 130(1):e2024JB029566, 2025. doi: 10.1029/2024JB029566.

Cogurcu, M. Construction and design defects in the residential buildings and observed earthquake damage types in Turkey. *Natural Hazards and Earth System Sciences*, 15(4):931–945, 2015. doi: 10.5194/nhess-15-931-2015.

Danciu, L., Nandan, S., Reyes, C., Basili, R., Weatherill, G., Beauval, C., Rovida, A., Vilanova, S., Sesetyan, K., Bard, P.-Y., Cotton, F., Wiemer, S., and Giardini, D. The 2020 update of the European Seismic Hazard Model - ESHM20: Model overview. Technical report, 2021. doi: 10.12686/a15.

Disaster and Emergency Management Authority. Turkish National Strong Motion Network, 1973. doi: 10.7914/SN/TK.

Disaster and Emergency Management Authority. Turkish National Seismic Network, 1990. doi: 10.7914/SN/TU.

Dziewonski, A. M., Chou, T.-A., and Woodhouse, J. H. Determination of earthquake source parameters from waveform data for studies of global and regional seismicity. *Journal of Geophysical Research: Solid Earth*, 86(B4):2825–2852, 1981. doi: 10.1029/JB086iB04p02825.

Eken, T., Bohnhoff, M., Bulut, F., Can, B., and Aktar, M. Crustal Anisotropy in the Eastern Sea of Marmara Region in Northwestern Turkey. *Bulletin of the Seismological Society of America*, 103 (2A):911–924, 2013. doi: 10.1785/0120120156.

Ekström, G., Nettles, M., and Dziewoński, A. The global CMT project 2004–2010: Centroid-moment tensors for 13,017 earthquakes. *Physics of the Earth and Planetary Interiors*, 200-201:1–9, 2012. doi: 10.1016/j.pepi.2012.04.002.

Emre, O., Duman, T. Y., Ozalp, S., Saroglu, F., Olgun, S., Elmaci, H., and Can, T. Active fault database of Turkey. *Bulletin of Earthquake Engineering*, 16(8):3229–3275, 2018. doi: 10.1007/s10518-016-0041-2.

Erdik, M., Demircioglu, M., Sesetyan, K., Durukal, E., and Siyahi, B. Earthquake hazard in Marmara region, Turkey. *Soil Dynamics and Earthquake Engineering*, 24(8):605–631, 2004. doi: 10.1016/j.soildyn.2004.04.003.

Erdik, M., Pınar, A., Kale, O., Altunel, E., Tümsa, D., Apaydın, N., undefinedomoglu, M., Sandıkkaya, M., and Güryuva, B. April 2025 magnitude 6.2 earthquake near Istanbul highlights strengths and weaknesses in seismic mitigation. *Temblor*, Sept. 2025. doi: 10.32858/temblor.368.

Ergin, M., Özalaybey, S., Aktar, M., and Yalcin, M. Site amplification at Avcılar, Istanbul. *Tectonophysics*, 391(1-4):335–346, 2004. doi: 10.1016/j.tecto.2004.07.021.

Ergintav, S., Reilinger, R. E., Çakmak, R., Floyd, M., Cakir, Z., Doğan, U., King, R. W., McClusky, S., and Özener, H. Istanbul's earthquake hot spots: Geodetic constraints on strain accumulation along faults in the Marmara seismic gap. *Geophysical Research Letters*, 41(16):5783–5788, 2014. doi: 10.1002/2014GL060985.

Ergintav, S., Floyd, M., Paradissis, D., Karabulut, H., Vernant, P., Masson, F., Georgiev, I., Konca, A. O., Dogan, U., King, R., and Reilinger, R. New geodetic constraints on the role of faults and blocks vs. distribute strain in the Nubia-Arabia-Eurasia zone of active plate interactions. *Turkish Journal of Earth Sciences*, 32 (3):Article 2, 2023. doi: 10.55730/1300-0985.1842.

Ertuncay, D., Simone Francesco, F., Büyükakpınar, P., and Onur, T. Dataset of 'Initial observations of 23 April 2025 Marmara Sea, Türkiye earthquake: ground motion, seismic source, and aftershock analysis' article [dataset], July 2025. doi: 10.5281/zenodo.16421725.

Frohlich, C., Riedesel, M. A., and Apperson, K. D. Note concerning possible mechanisms for non-double-couple earthquake sources. *Geophysical Research Letters*, 16(6):523–526, 1989. doi: 10.1029/GL016i006p00523.

GEOFON Data Centre. GEOFON Seismic Network, 1993. doi: 10.14470/TR560404.

Geological and Seismological Institute of Moldova. Moldova Digital Seismic Network, 2007. doi: 10.7914/SN/MD.

Got, J.-L., Fréchet, J., and Klein, F. W. Deep fault plane geometry inferred from multiplet relative relocation beneath the south flank of Kilauea. *Journal of Geophysical Research: Solid Earth*, 99 (B8):15375–15386, 1994. doi: 10.1029/94JB00577.

Gunes, O. Turkey's grand challenge: Disaster-proof building inventory within 20 years. *Case Studies in Construction Materials*, 2: 18–34, 2015. doi: 10.1016/j.cscm.2014.12.003.

Güzel, M. and Fraser, S. A magnitude 6.2 quake shakes Istanbul and injures more than 230 people, 2025. https://apnews.com/article/turkey-earthquake-istanbul-sea-marmara-magnitude-emergency-46f20a2c0b6fa3cad7634d28d1f7e5d7. [Accessed 04-07-2025].

Hasterok, D., Halpin, J., Collins, A., Hand, M., Kreemer, C., Gard, M., and Glorie, S. New maps of global geologic provinces and tectonic plates: global tectonics data and QGIS project file [dataset], Mar. 2022. doi: 10.5281/zenodo.6586972.

Heimann, S., Kriegerowski, M., Isken, M., Cesca, S., Daout, S., Grigoli, F., Juretzek, C., Megies, T., Nooshiri, N., Steinberg, A., Sudhaus, H., Vasyura-Bathke, H., Willey, T., and Dahm, T. Pyrocko - An open-source seismology toolbox and library. *GFZ Data Services*, 2017. doi: 10.5880/GFZ.2.1.2017.001.

Heimann, S., Isken, M., Kühn, D., Sudhaus, H., Steinberg, A., Vasyura-Bathke, H., Daout, S., Cesca, S., and Dahm, T. Grond - A probabilistic earthquake source inversion framework [software]. http://pyrocko.org/grond/docs/current/, 2018. doi: 10.5880/GFZ.2.1.2018.003.

Heimann, S., Vasyura-Bathke, H., Sudhaus, H., Isken, M. P., Kriegerowski, M., Steinberg, A., and Dahm, T. A Python framework for efficient use of pre-computed Green's functions in seismological and other physical forward and inverse source problems. *Solid Earth*, 10(6):1921–1935, 2019. doi: 10.5194/se-10-1921-2019.

Infantino, M., Mazzieri, I., Özcebe, A. G., Paolucci, R., and Stupazzini, M. 3D physics-based numerical simulations of ground motion in Istanbul from earthquakes along the Marmara segment of the North Anatolian fault. *Bulletin of the Seismological Society of America*, 110(5):2559–2576, 2020. doi: 10.1785/0120190235.

Institutions, M. P. P. Mediterranean Very Broadband Seismographic Network (MedNet) [Data set], 1990. doi: 10.13127/sd/fbbbtdtd6q.

IPGP Data Center. IPGP Data Center. https://doi.org/10.17616/R31NJN23, 2024. Editing status: 2024-10-15. Last accessed: 2025-08-10.

Jamalreyhani, M., Pousse-Beltran, L., Hassanzadeh, M., Sadat Arabi, S., Bergman, E. A., Shamszadeh, A., Arvin, S., Fariborzi, N., and Songhori, A. Co-seismic slip of the 18 April 2021 Mw 5.9 Genaveh earthquake in the South Dezful Embayment of Zagros (Iran) and its aftershock sequence. *Seismica*, 2(1), 2023. doi: 10.26443/seismica.v2i1.246.

Kale, Ö., Akkar, S., Ansari, A., and Hamzehloo, H. A ground-motion predictive model for Iran and Turkey for horizontal PGA, PGV, and 5% damped response spectrum: Investigation of possible regional effects. *Bulletin of the Seismological Society of America*, 105(2A):963–980, 2015. doi: 10.1785/0120140134.

Kandilli Observatory And Earthquake Research Institute, Boğaziçi University. Kandilli Observatory And Earthquake Research Institute (KOERI), 1971. doi: 10.7914/SN/KO.

Karabulut, H., Schmittbuhl, J., Özalaybey, S., Lengline, O., Kömeç-Mutlu, A., Durand, V., Bouchon, M., Daniel, G., and Bouin, M. Evolution of the seismicity in the eastern Marmara Sea a decade before and after the 17 August 1999 Izmit earthquake. *Tectonophysics*, 510(1-2):17–27, 2011. doi: 10.1016/j.tecto.2011.07.009.

Karabulut, H., Güvercin, S. E., Eskiköy, F., Konca, A. Ö., and Ergintav, S. The moderate size 2019 September M w 5.8 Silivri earthquake unveils the complexity of the Main Marmara Fault shear zone. *Geophysical Journal International*, 224(1):377–388, 2021. doi: 10.1093/gji/ggaa469.

Karabulut, S. and Özel, O. 3-D shear wave velocity structure beneath the European Side of Istanbul from seismic noise arrays analysis. *Geophysical Journal International*, 215(3):1803–1823, 2018. doi: 10.1093/gji/ggy370.

Karasözen, E., Büyükakpınar, P., Ertuncay, D., Havazlı, E., and Oral, E. A call from early-career Turkish scientists: seismic resilience is only feasible with "earthquake culture". *Seismica*, 2(3), 2023. doi: 10.26443/seismica.v2i3.1012.

Kenawy, M. and Pitarka, A. Performance assessment of near-fault buildings subjected to physics-based simulated earthquake ground motions with fling step. *Earthquake Spectra*, 41 (1):381–411, 2025. doi: 10.1177/87552930241285022.

Kilic, H., Tohumcu Özener, P., Yildirim, M., Özaydin, K., and Adatepe, Ş. Evaluation of Küçükçekmece region with respect to soil amplification. In *Proceedings of the 16th International Conference on Soil Mechanics and Geotechnical Engineering*, pages 2667–2672. IOS Press, 2005. doi: 10.3233/978-1-61499-656-9-2667.

Klin, P., Laurenzano, G., Barnaba, C., Priolo, E., and Parolai, S. Site amplification at permanent stations in northeastern Italy. *Bulletin of the Seismological Society of America*, 111(4):1885–1904, 2021. doi: 10.1785/0120200361.

Kuge, K. and Lay, T. Systematic non-double-couple components of earthquake mechanisms: The role of fault zone irregularity. *Journal of Geophysical Research: Solid Earth*, 99(B8): 15457–15467, 1994. doi: 10.1029/94JB00140.

Kühn, D., Heimann, S., Isken, M. P., Ruigrok, E., and Dost, B. Probabilistic Moment Tensor Inversion for Hydrocarbon-Induced Seismicity in the Groningen Gas Field, The Netherlands, Part 1: Testing. *Bulletin of the Seismological Society of America*, 110(5): 2095–2111, 2020. doi: 10.1785/0120200099.

Le Pichon, X., Şengör, A., Demirbağ, E., Rangin, C., Imren, C., Armijo, R., Görür, N., Çağatay, N., De Lepinay, B. M., Meyer, B., et al. The active main Marmara fault. *Earth and Planetary Science Letters*, 192(4):595–616, 2001. doi: 10.1016/S0012-821X(01)00449-6.

Loth, C. and Baker, J. W. A Spatial Cross-correlation Model of

Spectral Accelerations at Multiple Periods. *Earthquake Engineering & Structural Dynamics*, 42(3):397–417, Mar. 2013. doi: 10.1002/eqe.2212.

Loth, C. and Baker, J. W. Erratum: A Spatial Cross-correlation Model for Ground Motion Spectral Accelerations at Multiple Periods. *Earthquake Engineering & Structural Dynamics*, 49(3): 315–316, Mar. 2020. doi: 10.1002/eqe.3233.

Metz, M., Maleki Asayesh, B., Mohseni Aref, M., Jamalreyhani, M., Büyükakpınar, P., and Dahm, T. The July–December 2022 earthquake sequence in the southeastern Fars arc of Zagros mountains, Iran. *Seismica*, 2(2), 2023. doi: 10.26443/seismica.v2i2.953.

Morales-Beltran, M. Understanding 60 years of soft storey in Türkiye: an interdisciplinary perspective. *Natural Hazards*, pages 1–40, 2025. doi: 10.1007/s11069-025-07258-4.

National Institute for Earth Physics (NIEP Romania). Romanian Seismic Network, 1994. doi: 10.7914/SN/RO.

National Institute of Geophysics, Geodesy and Geography - BAS. National Seismic Network of Bulgaria, 1980. doi: 10.7914/SN/BS.

National Observatory of Athens, Institute of Geodynamics, Athens. National Observatory of Athens Seismic Network, 1975. doi: 10.7914/SN/HL.

Okay, H. B. and Özacar, A. A. A Novel VS 30 Prediction Strategy Taking Fluid Saturation into Account and a New VS 30 Model of Türkiye. *Bulletin of the Seismological Society of America*, 114(2): 1048–1065, 2024. doi: 10.1785/0120230032.

Özel, O., Cranswick, E., Meremonte, M., Erdik, M., and Safak, E. Site effects in Avcilar, west of Istanbul, Turkey, from strong-and weak-motion data. *Bulletin of the Seismological Society of America*, 92(1):499–508, 2002. doi: 10.1785/0120000827.

Öztürk, Y. K., Konca, A. O., and Özel, N. M. 3D Dynamic Rupture Simulations for the Potential Main Marmara Fault Earthquake in the Sea of Marmara Based on the Inter-Seismic Strain Accumulation. *Journal of Geophysical Research: Solid Earth*, 130(7): e2024JB029585, 2025. doi: 10.1029/2024JB029585.

Parsons, T., Toda, S., Stein, R. S., Barka, A., and Dieterich, J. H. Heightened odds of large earthquakes near Istanbul: an interaction-based probability calculation. *Science*, 288(5466): 661–665, 2000. doi: 10.1126/science.288.5466.661.

Picozzi, M., Strollo, A., Parolai, S., Durukal, E., Özel, O., Karabulut, S., Zschau, J., and Erdik, M. Site characterization by seismic noise in Istanbul, Turkey. *Soil Dynamics and Earthquake Engineering*, 29(3):469–482, 2009. doi: 10.1016/j.soildyn.2008.05.007.

Pyper Griffiths, J. H., Irfanoglu, A., and Pujol, S. Istanbul at the threshold: an evaluation of the seismic risk in Istanbul. *Earthquake Spectra*, 23(1):63–75, 2007. doi: 10.1193/1.2424988.

Reilinger, R., McClusky, S., Vernant, P., Lawrence, S., Ergintav, S., Cakmak, R., Ozener, H., Kadirov, F., Guliev, I., Stepanyan, R., et al. GPS constraints on continental deformation in the Africa-Arabia-Eurasia continental collision zone and implications for the dynamics of plate interactions. *Journal of Geophysical Research: Solid Earth*, 111(B5), 2006. doi: 10.1029/2005JB004051.

Rösler, B., Stein, S., and Spencer, B. When are Non-Double-Couple Components of Seismic Moment Tensors Reliable? *Seismica*, 2 (1), Mar. 2023. doi: 10.26443/seismica.v2i1.241.

Rösler, B., Stein, S., Ringler, A., and Vackář, J. Apparent Non-Double-Couple Components as Artifacts of Moment Tensor Inversion. *Seismica*, 3(1), Apr. 2024. doi: 10.26443/seismica.v3i1.1157.

Şahin, M., Yaltırak, C., Bulut, F., and Garagon, A. Stress change generated by the 2019 İstanbul–Silivri earthquakes along the complex structure of the North Anatolian Fault in the Marmara Sea. *Earth, Planets and Space*, 74(1):1–16, 2022. doi: 10.1186/s40623-022-01706-2.

Schmittbuhl, J., Karabulut, H., Lengliné, O., and Bouchon, M. Seismicity distribution and locking depth along the Main Marmara Fault, Turkey. *Geochemistry, Geophysics, Geosystems*, 17(3): 954–965, 2016. doi: 10.1002/2015GC006120.

Şengör, A., Tüysüz, O., Imren, C., Sakınç, M., Eyidoğan, H., Görür, N., Le Pichon, X., and Rangin, C. The North Anatolian fault: A new look. *Annu. Rev. Earth Planet. Sci.*, 33(1):37–112, 2005. doi: 10.1146/annurev.earth.32.101802.120415.

Somerville, P. G., Smith, N. F., Graves, R. W., and Abrahamson, N. A. Modification of empirical strong ground motion attenuation relations to include the amplitude and duration effects of rupture directivity. *Seismological research letters*, 68(1):199–222, 1997. doi: 10.1785/gssrl.68.1.199.

Stupazzini, M., Infantino, M., Allmann, A., and Paolucci, R. Physics-based probabilistic seismic hazard and loss assessment in large urban areas: A simplified application to Istanbul. *Earthquake Engineering & Structural Dynamics*, 50(1):99–115, 2021. doi: 10.1002/eqe.3365.

Tan, O. Long-term aftershock properties of the catastrophic 6 February 2023 Kahramanmaraş (Türkiye) earthquake sequence. *Acta Geophysica*, pages 1–18, 2024. doi: 10.1007/s11600-024-01419-y.

Tan, O., Karagöz, Ö., Ergintav, S., and Duran, K. The neglected Istanbul earthquakes in the North Anatolian Shear Zone: tectonic implications and broad-band ground motion simulations for a future moderate event. *Geophysical Journal International*, 233 (1):700–723, 2023. doi: 10.1093/gji/ggac477.

Tezcan, S. S., Kaya, E., Bal, I. E., and Özdemir, Z. Seismic amplification at Avcılar, Istanbul. *Engineering structures*, 24(5):661–667, 2002. doi: 10.1016/S0141-0296(02)00002-0.

Turhan, F., Acarel, D., Plicka, V., Bohnhoff, M., Polat, R., and Zahradník, J. Coseismic Faulting Complexity of the 2019 M w 5.7 Silivri Earthquake in the Central Marmara Seismic Gap, Offshore Istanbul. *Seismological Society of America*, 94(1):75–86, 2023. doi: 10.1785/0220220111.

Türker, E., Yen, M.-H., Pilz, M., and Cotton, F. Significance of Pulse-Like Ground Motions and Directivity Effects in Moderate Earthquakes: The Example of the M w 6.1 Gölyaka-Düzce Earthquake on 23 November 2022. *Bulletin of the Seismological Society of America*, 114(2):955–964, 2024. doi: 10.1785/0120230043.

TÜBITAK Marmara Research Center. MRC Earth and Marine Sciences Network, 2016. doi: 10.7914/SN/TB.

U.S. Geological Survey, Earthquake Hazards Program. Advanced National Seismic System (ANSS) Comprehensive Catalog of Earthquake Events and Products. https://doi.org/10.5066/F7MS3QZH, 2017. Accessed: 2025-08-06.

Wald, D. J. and Worden, C. B. ShakeMap Manual. U.S. Geological Survey, 2016. doi: 10.5066/F7D21VPQ.

Waldhauser, F. and Ellsworth, W. L. A double-difference earthquake location algorithm: Method and application to the northern Hayward fault, California. *Bulletin of the seismological society of America*, 90(6):1353–1368, 2000. doi: 10.1785/0120000006.

Worden, C. B., Gerstenberger, M. C., Rhoades, D. A., and Wald, D. J. Probabilistic Relationships between Ground-Motion Parameters and Modified Mercalli Intensity in California. *Bulletin of the Seismological Society of America*, 102(1):204–221, Feb. 2012. doi: 10.1785/0120110156.

Worden, C. B., Thompson, E. M., Baker, J. W., Bradley, B. A., Luco, N., and Wald, D. J. Spatial and Spectral Interpolation of Ground-

Motion Intensity Measure Observations. *Bulletin of the Seismological Society of America*, 108(2):866–875, Apr. 2018. doi: 10.1785/0120170201.

WorldPop and Bondarenko, M. Individual countries 1km UN adjusted population density (2000-2020), 2020.

Yakut, A., Sucuoğlu, H., and Akkar, S. Seismic risk prioritization of residential buildings in Istanbul. *Earthquake engineering & structural dynamics*, 41(11):1533–1547, 2012. doi: 10.1002/eqe.2215.

Yılmaz, Z., Konca, A. Ö., and Ergintav, S. The Effect of the 3-D Structure on Strain Accumulation and the Interseismic Behavior Along the North Anatolian Fault in the Sea of Marmara. *Journal of Geophysical Research: Solid Earth*, 127(3):e2021JB022838, 2022. doi: 10.1029/2021JB022838.

The article *23 April 2025 Marmara Sea (M_w 6.3), Türkiye earthquake: mainshock, aftershock, and ground observations* © 2025 by Deniz Ertuncay is licensed under CC BY 4.0.